HHS Public Access

Author manuscript

Int J Comput Assist Radiol Surg. Author manuscript; available in PMC 2016 December 01.

Published in final edited form as:

Int J Comput Assist Radiol Surg. 2015 December ; 10(12): 2009–2020. doi:10.1007/s11548-015-1255-5.

Intraoperative CT as a registration benchmark for intervertebral motion compensation in image-guided open spinal surgery

Songbai Ji[1,2], **Xiaoyao Fan**[1], **Keith D. Paulsen**[1,3], **David W. Roberts**[2,3], **Sohail K. Mirza**[2,3], and **S. Scott Lollis**[2,3]

Songbai Ji: Songbai.Ji@Dartmouth.edu

[1]Thayer School of Engineering, Dartmouth College, 14 Engineering Drive, Hanover, NH 03755, USA

[2]Geisel School of Medicine, Dartmouth College, Hanover, NH 03755, USA

[3]Dartmouth Hitchcock Medical Center, Lebanon, NH 03766, USA

Abstract

Purpose—An accurate and reliable benchmark of registration accuracy and intervertebral motion compensation is important for spinal image guidance. In this study, we evaluated the utility of intraoperative CT (iCT) in place of bone-implanted screws as the ground-truth registration and illustrated its use to benchmark the performance of intraoperative stereovision (iSV).

Methods—A template-based, multi-body registration scheme was developed to individually segment and pair corresponding vertebrae between preoperative CT and iCT of the spine. Intervertebral motion was determined from the resulting vertebral pair-wise registrations. The accuracy of the image-driven registration was evaluated using surface-to-surface distance error (SDE) based on segmented bony features and was independently verified using point-to-point target registration error (TRE) computed from bone-implanted mini-screws. Both SDE and TRE were used to assess the compensation accuracy using iSV.

Results—The iCT-based technique was evaluated on four explanted porcine spines (20 vertebral pairs) with artificially induced motion. We report a registration accuracy of 0.57 ± 0.32 mm (range 0.34–1.14 mm) and 0.29 ± 0.15 mm (range 0.14–0.78 mm) in SDE and TRE, respectively, for all vertebrae pooled, with an average intervertebral rotation of 4.9° ± 1.2° (range 1.5°–7.9°). The iSV-based compensation accuracy for one sample (four vertebrae) was 1.32 ± 0.19 mm and 1.72 ± 0.55 mm in SDE and TRE, respectively, exceeding the recommended accuracy of 2 mm.

Conclusion—This study demonstrates the effectiveness of iCT in place of invasive fiducials as a registration ground truth. These findings are important for future development of on-demand spinal image guidance using radiation-free images such as stereovision and ultrasound on human subjects.

Correspondence to: Songbai Ji, Songbai.Ji@Dartmouth.edu.

Conflict of interest: K.D. Paulsen and D.W. Roberts receive research support from Medtronic Inc. and Carl Zeiss Inc. D.W. Roberts serves on the scientific advisory board for Medtronic Inc., Carl Zeiss Inc., and IMRIS Inc. Other authors declare that they have no conflict of interest.

Keywords

Spinal surgery; Fusion surgery; Intervertebral motion; Motion compensation; Patient registration; Registration accuracy; Intraoperative CT

Introduction

Image guidance has become ubiquitous in cranial neuro-surgery for safe, effective, and minimally invasive procedures [1]. In spinal surgery, however, this technology has largely been limited to the placement of bone (pedicle) screws for lumbar stabilization in degenerative disease [2]. Despite studies showing that use of image guidance decreases vertebral screw misplacement [3–8], 60 % of spine surgeons never use image guidance, and only 11 % employ the technology on a regular basis [9]. Further, image guidance is rarely used in other types of spinal operations, such as tumor removal, deformity correction, or simple decompression.

Underutilization of image guidance in spinal surgery may be due to inefficient and often ineffective patient registration. Skin fiducials commonly used in cranial neurosurgery are not viable for patient registration in spinal surgery [10,11]. In practice, an experienced physician is often required to define, expose, and localize anatomic landmarks within the surgical field [12]. In addition, the one-time registration is ineffective because it does not account for intervertebral motion during spinal operations that could invalidate the initial registration accuracy. Since the anatomic landmarks may either become inaccessible or unavailable, a re-registration based on anatomic landmarks is typically infeasible. While intra-operative CT (iCT) or fluoroscopy can allow an updated patient registration, concerns about their radiation exposure limit their use. Their substantial cost further restricts a wider deployment [13].

Our research team is investigating low-cost, radiation-free intraoperative stereovision (iSV [14]) and three-dimensional (3D) ultrasound (iUS) to perform initial patient registration and intraoperative re-registration to compensate for intervertebral motion in spinal surgery (analogously to brain shift compensation in neurosurgery [15,16]). To this end, it is important to identify a reliable means to assess the registration accuracy in order to establish their clinical utility in human patients. Although screws or invasive fiducials can be implanted in phantoms and animals for research and validation purposes [17,18], the added invasiveness and risk of additional instrumentation for purely research purposes may not be justified in human patients. As an alternative, iCT that offers a complete volumetric sampling of the spinal region of interest may be used to serve as a ground truth to assess the registration accuracy. With sufficient and robust validation, radiation-free intraoperative images such as iSV and/or iUS might find widespread, routine use in clinical patient cases.

The goal of this study is to investigate the utility of iCT in place of invasive fiducials as a ground-truth benchmark registration. Explanted porcine spine phantoms were manually positioned in different configurations to simulate patient re-positioning due to posture changes and operative manipulation. Volumetric CT images were acquired before and after the reconfiguration (“preoperative” CT and iCT, respectively). A template-based multi-body

registration scheme was developed to segment and register individual vertebral pairs between the two poses. The resulting pair-wise, individual level registrations were then used to detect changes in relative vertebral pose, or effectively, intervertebral motion. The registration accuracy was evaluated in terms of SDE and TRE. The TRE was independently measured using bone-implanted mini-screws.

A quantitative comparison of iCT and traditional bone-implanted screws for serving as ground-truth registration has not been reported before, at least in spine surgery. Therefore, our current study represents a unique contribution to the field. Importantly, these investigations will facilitate our future studies to evaluate the utility of iSV and/or iUS for initial patient registration as well as intraoperative re-registration in human patients (illustrated using iSV for intervertebral motion compensation on one sample in this study). By comparing the registration transforms at the individual vertebral levels between iSV/iUS and pCT with those obtained between iCT and pCT, their registration accuracy can be directly established, without relying on invasive fiducials [17,18] or anatomic landmarks that are either infeasible or challenging to localize [19,20].

Materials and methods

Image acquisition

Following IACUC approval, four explanted porcine spines were obtained from animal research breeding facilities (weight range 35–70 kg). Lumbar vertebrae were surgically exposed. Four Leibinger titanium mini-screws (1.5 mm diameter, 3 mm depth) were implanted into each exposed vertebra to serve as fiducials for independent assessment of TRE [21]. Preoperative CT (pCT) images were acquired for each spine in a natural “prone” posture. Next, the spine posture was manually altered with a combination of bending, torsion, and/or extension to artificially induce intervertebral motion. A second set of “intraoperative” CT (iCT) images was then acquired. Immediately before each CT image acquisition, iSV and iUS images were also acquired to assess their utility in patient registration and intervertebral motion compensation. The iSV/iUS-related image processing or registrations with respect to pCT or iCT are not the focus of the current study and will be reported in detail separately in the future. Nevertheless, as an illustration in this study, we also employed iSV to compensate for intervertebral motion and compared its performance with respect to iCT and bone-implanted screws on one porcine sample. All CT images had a pixel resolution of 0.27 mm × 0.27 mm × 0.60 mm. All image acquisitions and surgical operations were conducted in the newly established Center for Surgical Innovation (CSI) at Dartmouth.

Image preprocessing

To improve the accuracy and robustness in image registration, CT images were preprocessed to highlight bony structures [17,22–24]. This included thresholding, erosion, identifying the largest connected region, and dilation (with an optimal kernel size of 2 determined for erosion and dilation). Since the same processing parameters were applied to both pCT and iCT, they were not anticipated to significantly influence the CT registrations. Figure 1a, b shows a typical pCT axial image before and after preprocessing to minimize artifacts and

soft tissues. Fiducial mini-screws (arrows, Fig. 1a, b) were automatically segmented via a simple thresholding, and their centroids were then identified in pCT and iCT. The implanted screws passively served as independent markers to report TRE at each individual vertebral level. A photographic image of an exposed spine captured in iSV is shown in Fig. 1c.

Template-based segmentation and pair-wise registration

Accurate vertebral segmentation and identification were important for spinal image guidance. Techniques to automatically detect, identify, and segment whole-column vertebral bodies include: spinal curve extraction using prior knowledge of shape, gradient, and appearance information models [25]; training bone-structure edge detection with a coarse-to-fine two-stage registration of a deformable surface model [26]; fully automatic methods based on deformable fences [27]; and the use of multi-vertebrae anatomic shape and pose models [28]. While all of these methods are effective, they may not be readily applicable to our study on porcine spines, due to interspecies morphological variation. To register pair-wise, identical vertebral bodies in two CT image volumes in this study, we devised a template-based registration to segment and pair the corresponding vertebrae.

Figure 2 illustrates the concept. A typical vertebra in pCT was first segmented as the volume contained by two manually defined axial planes, passing through two adjacent intervertebral discs. The resulting template vertebra was used to rigidly register with each segment of interest in both pCT and iCT (i.e., “one-to-many” registrations). Because the image-based registration performed optimization locally in parametric space, an appropriate initial starting point was provided prior to each registration (i.e., by placing the template volume along the spinal column direction multiple integer times of the typical vertebral height, approximately 25–40 mm). Upon registration convergence, the two defining axial planes were rigidly transformed accordingly to define/segment the vertebra of interest. Next, the identified vertebral pairs (see below) were further rigidly registered individually on a pair-wise basis (i.e., “one-to-one” registration). To ensure successful registration and minimize computational cost, an initial starting point was similarly provided to pre-align the vertebral centroids automatically identified in the two image volumes (i.e., using the centroid of all nonzero voxels in each segmented vertebra).

In order to ensure that the appropriate corresponding vertebrae were used for the pair-wise registration, their correct pairing was critical. For the spine, each vertebral body remained rigid regardless of the induced intervertebral motion between segments. While adjacent vertebrae were morphologically similar, still, they exhibited anatomic variations. Therefore, the converged error metric, based on an identical template vertebra in registration (i.e., “one-to-many” registration in Fig. 2), was expected to be sufficiently sensitive in identifying itself in both pCT and iCT. This concept is verified in Fig. 3, where the vertebra corresponding to the smallest error metric was correctly identified to be the selected template. Once the same template vertebra was localized in pCT and iCT, other corresponding vertebral pairs were easily identified.

The surface rendering of a typical porcine spine is shown in Fig. 4a, along with the template vertebra. The individually segmented and uniquely paired vertebrae in pCT and iCT are shown in Fig. 4b, c, showing a lateral bending/torsion-dominated motion for this specimen.

Intervertebral motion compensation using pCT

For two arbitrary adjacent vertebrae (e.g., *i* th and (*i* +1)st levels), the two independent pair-wise rigid registrations (e.g., T_i and $T_{(i+1)}$, respectively; Fig. 5) were obtained to optimally align each corresponding vertebral pair between pCT and iCT. Using T_i, both the *i* th and (*i* + 1)st vertebrae could be rigidly transformed into iCT; the transformed (*i* + 1)st vertebra served as a reference pose when no intervertebral motion occurred. On the other hand, $T_{(i+1)}$ determined its actual pose after compensating for its relative motion. Therefore, the pose change in the (*i* + 1)st vertebra relative to the *i* th vertebra between pCT and iCT, or equivalently, the relative motion of the two adjacent vertebrae, can be directly determined following the relationship below:

$$^{i}T_{i+1} = T_i \times \mathrm{inv}(T_{i+1}). \quad (1)$$

Conceptually, this strategy first transformed the (*i* +1)st vertebra in iCT into the pCT image space (following inv(T_i +1)) and then further into the iCT image space following the transformation determined from the pair-wise registration of the *i* th vertebra shown in Fig. 5 (i.e., T_i)' thereby avoiding an unnecessary additional registration.

Intervertebral motion compensation using iSV

Combining and resampling multiple iSV reconstructed surfaces—We further used porcine spine specimen #2 to illustrate the use of iSV for intervertebral motion compensation, and to benchmark its performance against iCT and bone-implanted screws. The iSV acquisitions were individually reconstructed into 3D geometrical surfaces using an optical-flow correspondence matching technique [29]. Because all iSV acquisitions were tracked, the reconstructed surfaces were transformed into the common coordinate system of the patient tracker rigidly attached to the spine. The overlapping surfaces were combined and resampled via projection images, analogously to that applied to the brain [29,30].

First, a local coordinate system was created with its origin located at the centroid of the reconstructed surface nodal positions while the *z*-axis along the spinal inferior-to-superior direction. The *x*- and *y*-axes were subsequently determined along the lateral and ventral-to-dorsal directions of the spine. Next, a 2D mesh was created in the *xz*-plane with a nodal density of 0.5 mm per pixel in both directions. The mesh physical dimensions, and hence, the image size, were determined from the combined iSV sampling area. For each reconstructed iSV surface, nodal positions were projected into the *xz*-plane with their *y*-coordinates assigned to the closest mesh nodes. For each mesh node, multiple assignments were possible due to sampling overlap, and they were averaged to produce a unique value representing the dorsal surface "height" in the ventral–dorsal direction. The algorithm was repeated for all iSV reconstructed surfaces. Because the topological intensity values were averaged at a predetermined set of mesh nodes, multiple iSV acquisitions were easily combined (Fig. 6). The iSV 3D-to-2D projection was numerically invertible because the corresponding 3D coordinate for each 2D image pixel (and vice versa) was uniquely determined as long as the surfaces were free of "image folding" (average coordinate in the overlapping region).

Intervertebral motion detection—Patient registration in spine surgery can be directly established by registering tracked iSV and pCT, as reported elsewhere [14]. For simplicity, here we employed the ground-truth registrations obtained from the bone-implanted screws via the Medtronic StealthStation to transform iSV reconstructed surfaces into the pCT or iCT image space, respectively, at the two imaging stages. Ten (N = 10) ordered bone-implanted screws were localized in pCT/iCT and the OR. Patient registrations were established separately before and after inducing the intervertebral motion following the standard procedure via the StealthStation. The combined and resampled iSV point clouds were then transformed into their respective pCT or iCT image space.

A two-step approach was used to achieve pair-wise vertebral registrations using iSV. First, points from the co-registered and resampled iSV surface corresponding to the vertebra of interest were first localized based on the individually segmented pCT or iCT via closest point search (e.g., points within 5 mm relative to the pCT/iCT isosurface of the vertebra; L4 in Fig. 6). The two subset point clouds were registered to generate an initial starting point for the next refined registration between the subset in pCT and the entire iSV point cloud in iCT (the latter serving as “stationary”), both via an improved ICP algorithm [31]. Concatenating the two registration transforms completed the iSV-based vertebral pair-wise registrations.

The accuracy of the iSV-based registration was assessed in terms of SDE between the two iSV surface point clouds for each vertebra upon final convergence (i.e., subset in pCT vs. entire surface in iCT). In addition, screw locations in pCT of the corresponding vertebra were transformed into the iCT image space to compute point-wise TRE. These measures were compared with those obtained from iCT-based registrations (SDE evaluated using vertebral isosurface from pCT and iCT upon registration convergence).

Data analysis

All image registrations were performed in ITK via minimizing the mean-squared differences in intensity, since all images had similar intensity ranges. All geometrical surface registrations were performed using an improved ICP algorithm [31]. With proper initial starting points, all registrations converged successfully (typically within 10 or 30 s for image or surface registrations, respectively). Registration accuracy was evaluated in terms of average SDE between two 3D point clouds of each individually segmented vertebra (with point density of approximately 0.5 mm). Using each pair-wise, image-based registration, TRE based on the bone-implanted fiducials was also independently computed. To assess the effectiveness of the pair-wise registration at the individual vertebral level, SDEs and TREs without incorporating individual level pair-wise registrations were also reported and compared (i.e., by only rigidly aligning L1 in pCT and iCT using the corresponding pair-wise registration, T_1, to avoid an arbitrary rigid body misalignment). For each spine, Pearson correlation was performed between the SDE and TRE (significance was defined at p = 0.05). Magnitudes of relative vertebral rotations were also reported. Finally, the registration accuracies from iSV were compared with those from iCT in terms of SDE and TRE. All image processing and data analyses were performed on a Windows computer with

dual octo-cores (Intel Xeon E5-2650, 2.6 GHz, 32 GB RAM) using MATLAB (R2014a, The Mathworks, Natick, MA, USA).

Results

Figure 7 demonstrates the effectiveness of iCT-based individual level pair-wise registrations for specimen #1. Vertebral alignments in terms of bony surfaces and bone-implanted screws significantly improved after the pair-wise registrations were applied (Fig. 7b), despite imperfect segmentations (some parts of the vertebral bony edges were missing in iCT).

For two selected porcine spines (specimens 1 and 2), the cross sections of the bony structures on a mid-sagittal plane (defined in iCT) are also compared before and after applying pair-wise registrations (Figs. 8, 9). Without motion compensation, the vertebral cross sections were consistent with the induced motion for both spines, which was either rotation/torsion (Fig. 8d) or extension (Fig. 9d) dominated for the two porcine spines. After motion compensation, the cross sections for all vertebrae based on the updated pCT were nearly identical to those in iCT in terms of shape and spinal curvature (Figs. 8e, f, 9e, f).

Quantitative SDEs and TREs using the single-level registration, T_1, or individual pair-wise registrations, T_i, are compared in Fig. 10. Without intervertebral motion compensation, both SDE and TRE increased with the increase in the distance relative to L1 that served as the alignment reference, and their values were highly and statistically correlated (correlation coefficient > 0.99; $p < 0.005$). After motion compensation using T_i, both SDE and TRE were substantially reduced. For all vertebral samples pooled, the average SDE and TRE were 0.57 ± 0.32 mm (range 0.34–1.14 mm) and 0.29 ± 0.15 mm (range 0.14–0.78 mm), respectively. However, no statistically significant correlations existed between the two measures in this case (p range 0.26–0.88).

The relative intervertebral rotations detected from the pCT-to-iCT pair-wise registrations are reported in Table 1. The average was 4.9° ± 1.2° (range 1.5°–7.9°), for all vertebrae pooled.

Figure 11 visually compares the effectiveness of iSV in intervertebral motion compensation against that from iCT. Screw locations identified in pCT were transformed using either the iSV- or iCT-based individual level pair-wise registrations. They aligned well with their iCT counterparts. The registration accuracies in terms of SDE and TRE are reported in Table 2.

Discussion

Maintaining sufficient registration accuracy at the individual vertebral level is important for effective image guidance throughout spinal surgery. Potentially, radiation-free iSV/iUS can be employed on an on-demand basis to provide an updated image guidance whenever needed. Nevertheless, a ground-truth benchmark is necessary and important to establish their clinical utility in human patients.

In this study, we evaluated the feasibility of using iCT as a ground-truth registration benchmark in the context of intervertebral motion compensation in spine surgery. A simple, yet effective template-based registration scheme was developed via pair-wise pCT-to-iCT

registrations. Specifically, the technique first automatically segmented and then paired each corresponding vertebra in pCT and iCT by exploiting both (1) the morphological similarity as well as variation between adjacent vertebral segments, and (2) the fact that the multi-body spinal vertebrae remain rigid after re-positioning. Lumbar vertebrae were automatically segmented in both pCT and iCT by rigidly registering each segment of interest with a single template. The individually segmented vertebrae in pCT and iCT were uniquely paired based on the converged registration error metric values. Because the template vertebra was chosen directly from the existing spinal vertebrae, the converged registration error metric was found to be minimal when registering with itself. The error metric monotonically increased when registering with vertebrae further away from the template vertebra, as expected (Fig. 3), presumably because of greater morphological differences.

The template vertebra in this study was manually defined based on the spinal column morphology in pCT via two axial imaging planes passing through the adjacent discs. Because it was *approximately* defined in our study, segmentations of other vertebrae were similarly approximate and may inevitably include unwanted features from adjacent vertebrae or missing part of the features from the vertebra of interest. Nevertheless, an automatic registration-based segmentation, pairing, and unique identification [25] may be attainable with a vertebral shape model [28]. Incorporating deformable (vs. rigid in this study) image registration with local rigidity constraints could also improve the performance [32], albeit its long runtime (hours or 10 min with trade-off between efficiency and accuracy) could be a concern for clinical use.

Regardless, the resulting pair-wise pCT-to-iCT registrations were highly accurate and robust for all vertebral pairs evaluated (20 vertebrae in total from four porcine spines). All registrations achieved a sub-voxel accuracy of ~0.5 mm in terms of SDE based on surface point clouds (Fig. 10; voxel diagonal length of 0.71 mm). This was further verified via TRE independently measured from bone-implanted screws, where an even superior accuracy of ~0.2 mm was achieved (Fig. 10). The larger SDE values may have been, in part, a result of segmentation variations of the bony structures in the two image volumes, as shown in Fig. 7b (part of the transverse processes missing in pCT). Nevertheless, both measures were significantly superior to that achieved in iUS-to-CT registrations for porcine spine (1.6 mm [18]) or in patients (mean TRE of 1.2 mm with a maximum point error of 4.6 mm [20]). In addition, the registration scheme was also highly efficient (<10 s to converge successfully for all image registrations performed; compared to 2 min in [18] and 1–3 min in [20]). These results clearly suggest that the iCT-, template-based technique developed in this study was highly effective for intervertebral motion compensation (Figs. 7, 8, 9). On the other hand, when no intervertebral motion was compensated for (i.e., using a single-level vertebral registration to align the spine to avoid an arbitrary rigid misalignment; Figs. 8a, d and 9a, d), large registration errors were evident in terms of both SDE and TRE. Significant intervertebral motion accumulation was evident as larger errors were observed for vertebrae further away from the arbitrarily chosen reference, L1 (Fig. 10). Interestingly, the two registration error metrics were highly and significantly correlated ($p < 0.005$) in this case. These findings, once again, suggest that the SDE based on two point clouds, alone, may be

sufficiently indicative of the registration performance relative to the traditional point-based TRE, regardless of the registration status (successful or failed) for vertebral bony structures.

Previous studies in cranial neurosurgery have found that SDE, alone, is insufficient to assess registration performance for the brain, where significant, un-captured lateral shifts [33,34] could occur. Therefore, they strongly support the use of TRE over SDE. However, our current study suggests that for spinal applications, SDE and TRE provide concordant assessments of registration performance. The disparate results between spine and brain studies are likely attributed to the basic anatomic differences: The spine presents a rich and heterogeneous 3D topography, whereas the brain exhibits a relatively smooth and monotonous curvature.

The relative rotations between two adjacent vertebrae were also recovered from pair-wise vertebral registrations. Obviously, the relative rotational magnitude (Table 1), itself, was not sufficient to capture the full 3D relative motion. However, because the transformation matrix (Eq. 1) completely defined the relative motion, a full description could be easily obtained (e.g., in terms of relative rotation about all the three major axes; [35]), if so desired.

Importantly, these investigations on the use of iCT established its feasibility to replace traditional invasive bone-implanted screws for performance benchmark of other radiation-free, low-cost intraoperative images such as iSV and iUS in human patients in the future. Because the iCT-based SDE and fiducial-based TRE were both within sub-millimeter, either one could be sufficiently accurate to characterize the performance of iSV/iUS. By comparing the registration transforms between iSV/iUS and pCT with the ground truths established between iCT and pCT directly, the accuracy of patient registration can be readily obtained at each individual vertebral level. Further, the potential of automatic segmentation of vertebrae from pCT may obviate the need for their segmentation in iSV/iUS, which would likely be more challenging in practice [17–20].

Indeed, based on results from one porcine spine sample in this study, the iSV was able to achieve a millimeter accuracy in terms of surface-based SDE and point-based TRE (Table 2), exceeding the recommended accuracy of 2 mm [1]. The iSV-based TRE in L4 was notably larger (2.52 mm; Table 2), which was likely a result of the relative incomplete iSV sampling for this specific segment (Fig. 6a). Certainly, more extensive evaluations are needed to fully establish the clinical utility of iSV/iUS in terms of registration accuracy, efficiency and robustness throughout spinal surgery, which will be explored and reported in the future. Nevertheless, the iSV performance achieved here suggest the potential for this line of research.

Finally, an important limitation of our current study is that it was restricted to changes in spinal posture only. Motion compensation is likely more challenging at later surgical stages, after significant bone removal, pedicle screw or cage insertion, or deformity correction. Therefore, further research is necessary to assess the utility of iCT and ultimately, radiation-free intraoperative images such as iSV/iUS, for individual level registration and motion compensation at these more challenging, later stages. If radiation-free intra-operative images readily achieve an accurate and efficient patient registration and re-registration on-demand,

they will likely broaden the use of spinal navigation within the surgical community, and further expand its applications.

Conclusion

The current study demonstrates the feasibility of iCT to serve as a ground-truth registration benchmark in place of invasive fiducials. The template-based, multi-body registration scheme was sufficiently accurate, efficient, and robust to compensate for intervertebral motion due to posture changes. The resulting surface-based registration accuracy was consistent with point-based target registration error, supporting the use of iCT as ground truth to benchmark registration accuracy of other radiation-free imaging techniques such as iSV and iUS, as illustrated. Future studies may include more extensive assessment of the technique in later surgical stages when bone removal, pedicle screw insertion, or instrumentation occurs.

Acknowledgments

This work was supported, in part, by the NIH R21 NS078607, The Dartmouth Clinical and Translational Science Institute under Award Number KL2TR001088 from the National Center for Advancing Translational Sciences (NCATS) of the NIH (SJ), and the Dow-Crichlow Award (SSL). The content is solely the responsibility of the author(s) and does not necessarily represent the official views of Dartmouth SYNERGY or the NIH. The authors are grateful to Dr. Timothy Schaewe for technical assistance on SteathLink® and help from the Medtronic Navigation (Louisville, CO, USA).

References

1. Cleary K, Peters TM. Image-guided interventions: technology review and clinical applications. Annu Rev Biomed Eng. 2010; 12:119–142. [PubMed: 20415592]
2. Deyo RA, Nachemson A, Mirza SK. Spinal-fusion surgery—the case for restraint. Spine J. 2004; 4:138S–142S.
3. Holly LT. Image-guided spinal surgery. Int J Med Robot Comput Assist Surg. 2006; 2(January):7–15.
4. Tjardes T, Shafizadeh S, Rixen D, Paffrath T, Bouillon B, Stein-hausen ES, Baethis H. Image-guided spine surgery: state of the art and future directions. Eur Spine J. 2010; 19(1):25–45. [PubMed: 19763640]
5. Tian N-F, Huang Q-S, Zhou P, Zhou Y, Wu R-K, Lou Y, Xu H-Z. Pedicle screw insertion accuracy with different assisted methods: a systematic review and meta-analysis of comparative studies. Eur Spine J. 2011; 20(6):846–859. [PubMed: 20862593]
6. Gelalis ID, Paschos NK, Pakos EE, Politis AN, Arnaoutoglou CM, Karageorgos AC, Ploumis A, Xenakis Ta. Accuracy of pedicle screw placement: a systematic review of prospective in vivo studies comparing free hand, fluoroscopy guidance and navigation techniques. Eur Spine J. 2012; 21(2):247–255. [PubMed: 21901328]
7. Jost, GF.; Yonemura, KS.; Von Jako, RA. Intraoperative imaging and image-guided therapy. In: Jolesz, FA., editor. Intraoperative imaging and image-guided therapy. Springer; New York: 2014. p. 613-628.
8. Tormenti MJ, Kostov DB, Gardner Pa, Kanter AS, Spiro RM, Okonkwo DO. Intraoperative computed tomography image-guided navigation for posterior thoracolumbar spinal instrumentation in spinal deformity surgery. Neurosurg Focus. 2010; 28(3):E11. [PubMed: 20192656]
9. Härtl R, Lam KS, Wang J, Korge A, Kandziora F, Audigé L. Worldwide survey on the use of navigation in spine surgery. World Neurosurg. 2013; 79(1):162–172. [PubMed: 22469525]

10. Roessler K, Ungersboeck K, Dietrich W, Aichholzer M, Hittmeir K, Matula C, Czech T, Koos W. Frameless stereotactic guided neurosurgery: clinical experience with an infrared based pointer device navigation system. Acta Neurochir. 1997; 139(6):551–559. [PubMed: 9248590]
11. Brodwater B, Roberts D, Nakajima T, Friets E, Strohbehn J. Extracranial application of the frameless stereotactic operating microscope: experience with lumbar spine. Neurosurgery. 1993; 32(2):209–213. [PubMed: 8437658]
12. Nottmeier EW. A review of image-guided spinal surgery. J Neurosurg Sci. 2012; 56:35–47. [PubMed: 22415381]
13. Mirza SK, Wiggins GC, Kuntz C, York JE, Bellabarba C, Knonodi Ma, Chapman JR, Shaffrey CI. Accuracy of thoracic vertebral body screw placement using standard fluoroscopy, fluoroscopic image guidance, and computed tomographic image guidance: a cadaver study. Spine (Phila Pa 1976). 2003; 28(4):402–413. [PubMed: 12590219]
14. Ji S, Fan X, Paulsen K, Roberts D, Mirza SK, Lollis SS. Patient registration using intraoperative stereovision in image-guided open spinal surgery. IEEE Trans Biomed Eng. 201510.1109/TBME.2015.2415731
15. Ji, S.; Fan, X.; Roberts, DW.; Hartov, A.; Schaewe, TJ.; Simon, DA.; Paulsen, KD. Brain shift compensation via intraoperative imaging and data assimilation. In: Neu, C.; Genin, G., editors. CRC handbook of imaging in biological mechanics. CRC Press; Boca Raton: 2014. p. 229-240.
16. Ji S, Wu Z, Hartov A, Roberts DW, Paulsen KD. Mutual-information-based image to patient re-registration using intra-operative ultrasound in image-guided neurosurgery. Med Phys. 2008; 35(10):4612. [PubMed: 18975707]
17. Yan CXB, Goulet B, Chen SJ-S, Tampieri D, Collins DL. Validation of automated ultrasound-CT registration of vertebrae. Int J Comput Assist Radiol Surg. 2012; 7(4):601–610. [PubMed: 22113426]
18. Yan CXB, Goulet B, Pelletier J, Chen SJ-S, Tampieri D, Collins DL. Towards accurate, robust and practical ultrasound-CT registration of vertebrae for image-guided spine surgery. Int J Comput Assist Radiol Surg. 2011; 6(4):523–537. [PubMed: 20976567]
19. Rasoulian, A.; Osborn, J.; Sojoudi, S.; Nouranian, S.; Lessoway, VA.; Rohling, RN.; Abolmaesumi, P. A system for ultrasound-guided spinal injections? A feasibility study. IPCAI; 2014. p. 90-99.
20. Nagpal, S.; Hacihaliloglu, I.; Ungi, T.; Rasoulian, A.; Osborn, J.; Lessoway, Va; Rohling, RN.; Borschneck, DP.; Abolmaesumi, P.; Mousavi, P. A global CT to US registration of the lumbar spine. IPCAI; 2014. p. 108-117.
21. West JB, Fitzpatrick JM, Sa Toms, Maurer CR, Maciunas RJ. Fiducial point placement and the accuracy of point-based, rigid body registration. Neurosurgery. 2001; 48(4):810–816. discussion 816–817. [PubMed: 11322441]
22. Winter S, Brendel B, Pechlivanis I, Schmieder K, Igel C. Registration of CT and intraoperative 3-D ultrasound images of the spine using evolutionary and gradient-based methods. IEEE Trans Evol Comput. 2008; 12(3):284–296.
23. Lang A, Mousavi P, Gill S, Fichtinger G, Abolmaesumi P. Multi-modal registration of speckle-tracked freehand 3D ultrasound to CT in the lumbar spine. Med Image Anal. 2012; 16(3):675–686. [PubMed: 21982123]
24. Gill S, Abolmaesumi P, Fichtinger G, Boisvert J, Pichora D, Borsh-neck D, Mousavi P. Biomechanically constrained groupwise ultrasound to CT registration of the lumbar spine. Med Image Anal. 2012; 16(3):662–674. [PubMed: 21126904]
25. Klinder T, Ostermann J, Ehm M, Franz A, Kneser R, Lorenz C. Automated model-based vertebra detection, identification, and segmentation in CT images. Med Image Anal. 2009; 13(3):471–482. [PubMed: 19285910]
26. Ma, J.; Lu, L.; Zhan, Y.; Zhou, X. Hierarchical segmentation and identification of thoracic vertebra using learning-based edge detection and coarse-to-fine deformable model. MICCAI; 2010. p. 19-27.
27. Kim Y, Kim D. A fully automatic vertebra segmentation method using 3D deformable fences. Comput Med Imaging Graph. 2009; 33:343–352. [PubMed: 19328651]

28. Rasoulian A, Member S, Rohling R, Member S. Lumbar spine segmentation using a statistical multi-vertebrae anatomical shape + pose model. IEEE Trans Med Imaging. 2013; 32(10):1890–1900. [PubMed: 23771318]

29. Ji S, Fan X, Roberts DW, Hartov A, Paulsen KD. Cortical surface shift estimation using stereovision and optical flow motion tracking via projection image registration. Med Image Anal. 2014; 18(7):1169–1183. [PubMed: 25077845]

30. Sinha TK, Dawant BM, Duay V, Cash DM, Weil RJ, Thompson RC, Weaver KD, Miga MI. A method to track cortical surface deformations using a laser range scanner. IEEE Trans Med Imaging. 2005; 24(6):767–781. [PubMed: 15959938]

31. Kjer, HM.; Wilm, J. Evaluation of surface registration algorithms for PET motion correction. Technical University of Denmark; 2010.

32. Reaungamornrat S, Wang aS, Uneri a, Otake Y, Khanna aJ, Siewerdsen JH. Deformable image registration with local rigidity constraints for cone-beam CT-guided spine surgery. Phys Med Biol. 2014; 59(14):3761–3787. [PubMed: 24937093]

33. Fan, X.; Ji, S.; Hartov, A.; Roberts, D.; Paulsen, K. Registering stereovision surface with preoperative magnetic resonance images for brain shift compensation. Proceedings of SPIE, medical imaging 2012: visualization, image-guided procedures, and modeling; 2012.

34. Paul P, Morandi X, Jannin P. A surface registration method for quantification of intraoperative brain deformations in image-guided neurosurgery. IEEE Trans Inf Technol Biomed. 2009; 13(6): 976–983. [PubMed: 19546046]

35. Fujii R, Sakaura H, Mukai Y, Hosono N, Ishii T, Iwasaki M, Yoshikawa H, Sugamoto K. Kinematics of the lumbar spine in trunk rotation: in vivo three-dimensional analysis using magnetic resonance imaging. Eur Spine J. 2007; 16(11):1867–1874. [PubMed: 17549527]

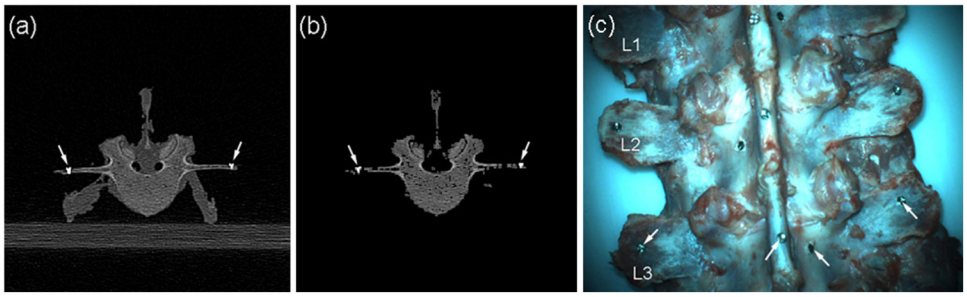

Fig. 1.

A typical axial CT image of the spine before (**a**) and after (**b**) image preprocessing, along with a photographic view of the phantom (**c**). *Arrows* indicate locations of implanted mini-screws passively serving as independent fiducials

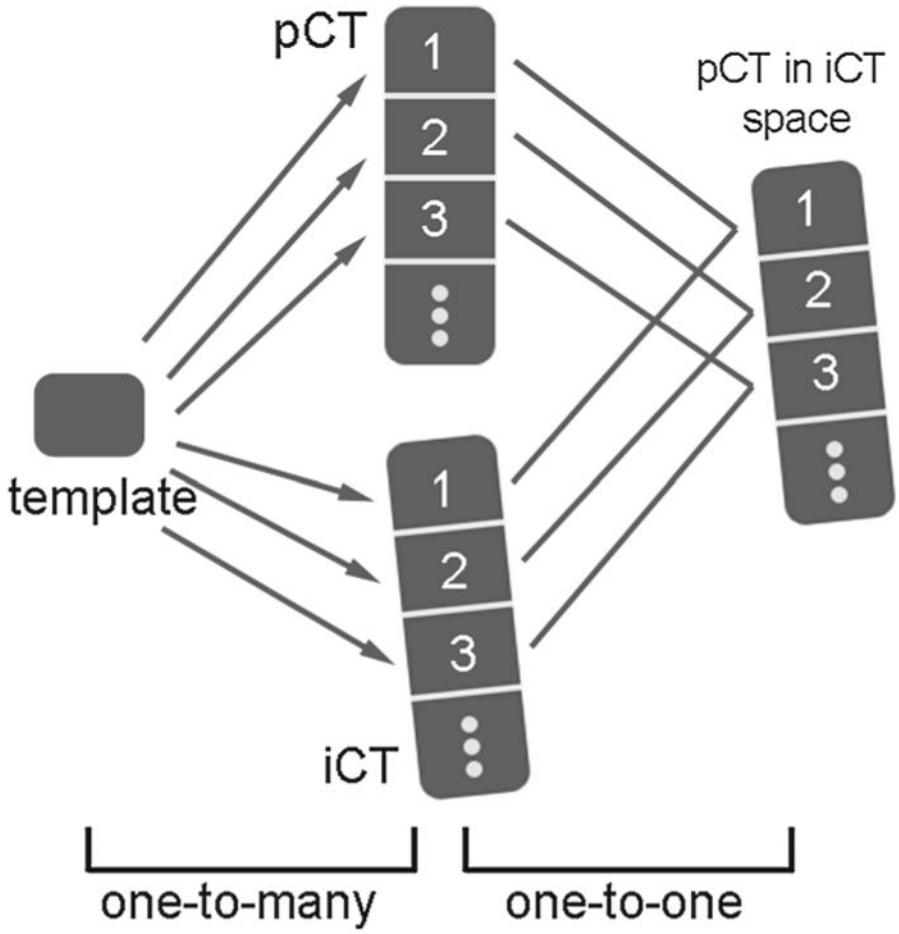

Fig. 2.

Schematic of the template-based, multi-body rigid registration to individually segment each vertebra and perform pair-wise registrations between their corresponding pairs

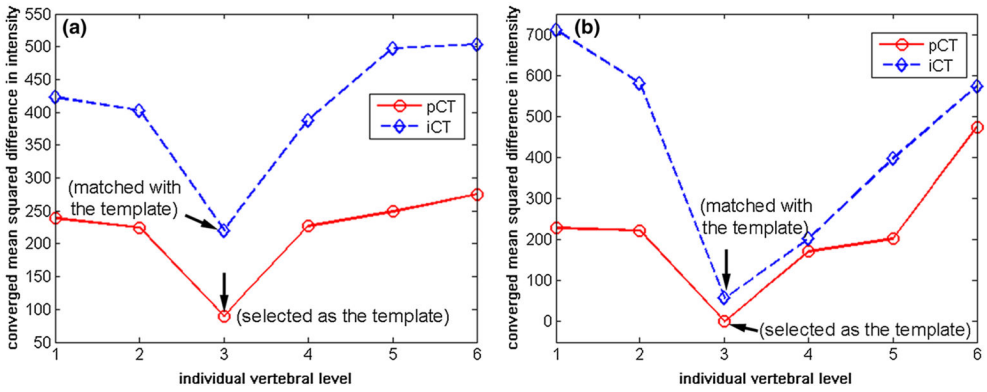

Fig. 3.

Converged error metric values between the template vertebra and each individually segmented vertebra in pCT and iCT for the two porcine spines **a** and **b**. When the template vertebra matched with itself, the converged error metric reached the minimum, which allowed correct pairing between pCT and iCT. All other corresponding vertebrae can then be uniquely paired

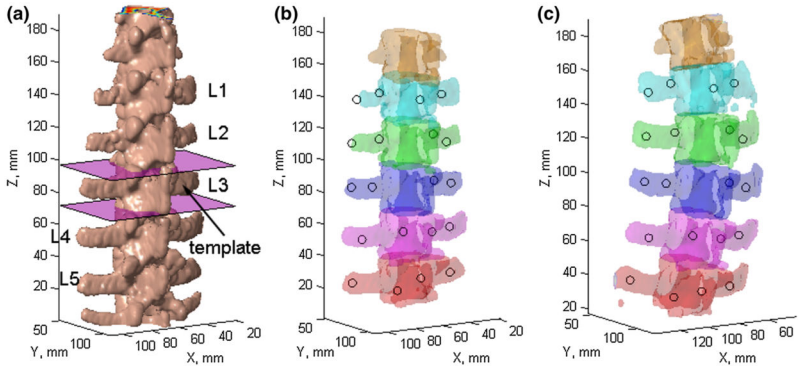

Fig. 4.

Surface rendering of the vertebral bodies in pCT (**a**) as well as the individually segmented and paired vertebrae (*with identical color*) in pCT (**b**) and iCT (**c**) for spine sample #1. The template vertebra in **a** was defined by two axial planes manually placed passing through the adjacent intervertebral discs. The locations of the automatically segmented mini-screws are also shown (*circles* in **b** and **c**)

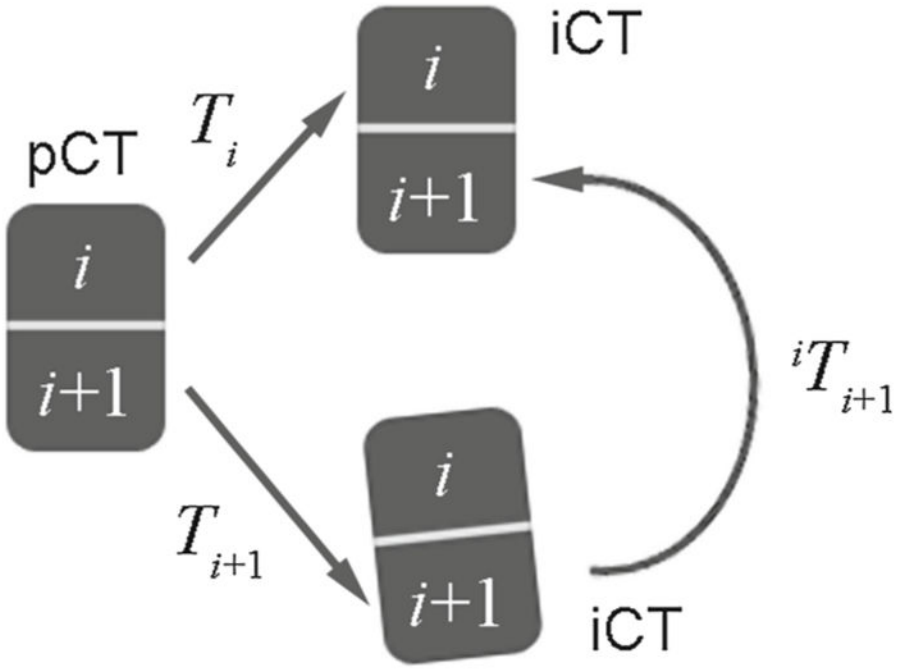

Fig. 5.

Conceptual illustration of transformation between two adjacent vertebrae due to pose change between pCT and iCT as a result the difference in two rigid body registrations

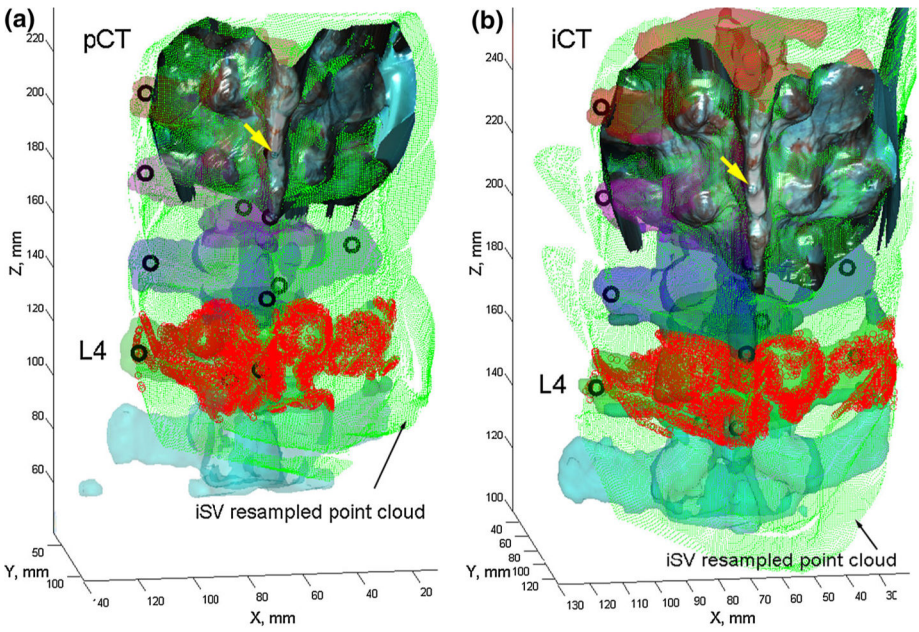

Fig. 6.

Individually segmented and color-coded vertebrae in pCT (**a**) and iCT (**b**) overlaid with the uniformly resampled iSV point cloud as well as the implanted mini-screws (*black circles*). A typical reconstructed iSV texture surface is also shown. For illustration, the iSV point clouds corresponding to L4 are *highlighted*

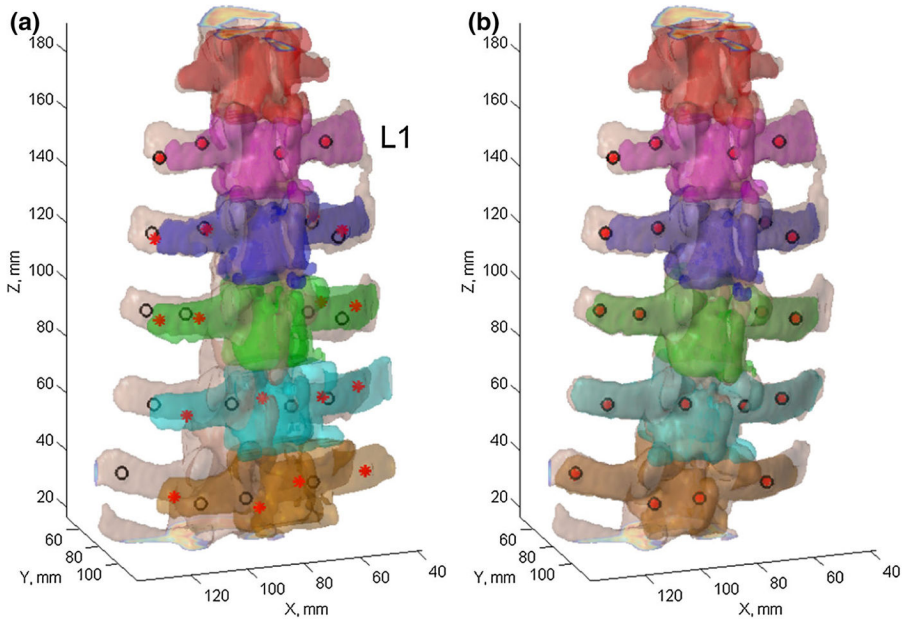

Fig. 7.

Individually segmented and paired vertebrae from pCT and iCT using registration from L1 (**a**) or pair-wise registrations (**b**) for alignment, along with their corresponding locations of bone-implanted mini-screws independently identified

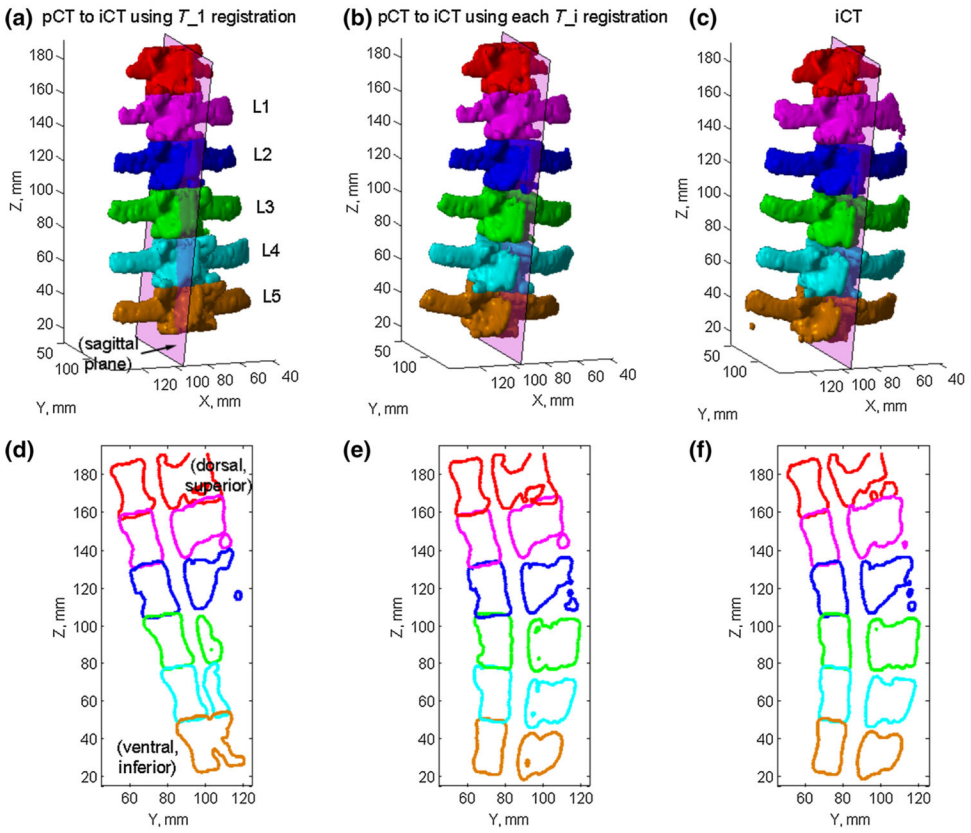

Fig. 8.

Individually segmented and paired vertebrae in pCT transformed into the iCT space by only aligning L1 in the two image volumes (**a**) or by aligning each corresponding vertebra using pair-wise registrations (**b**), and are compared with their iCT counterparts (**c**) for spine sample #1. Their corresponding cross sections on a sagittal plane defined in iCT are compared in **d**–**f**

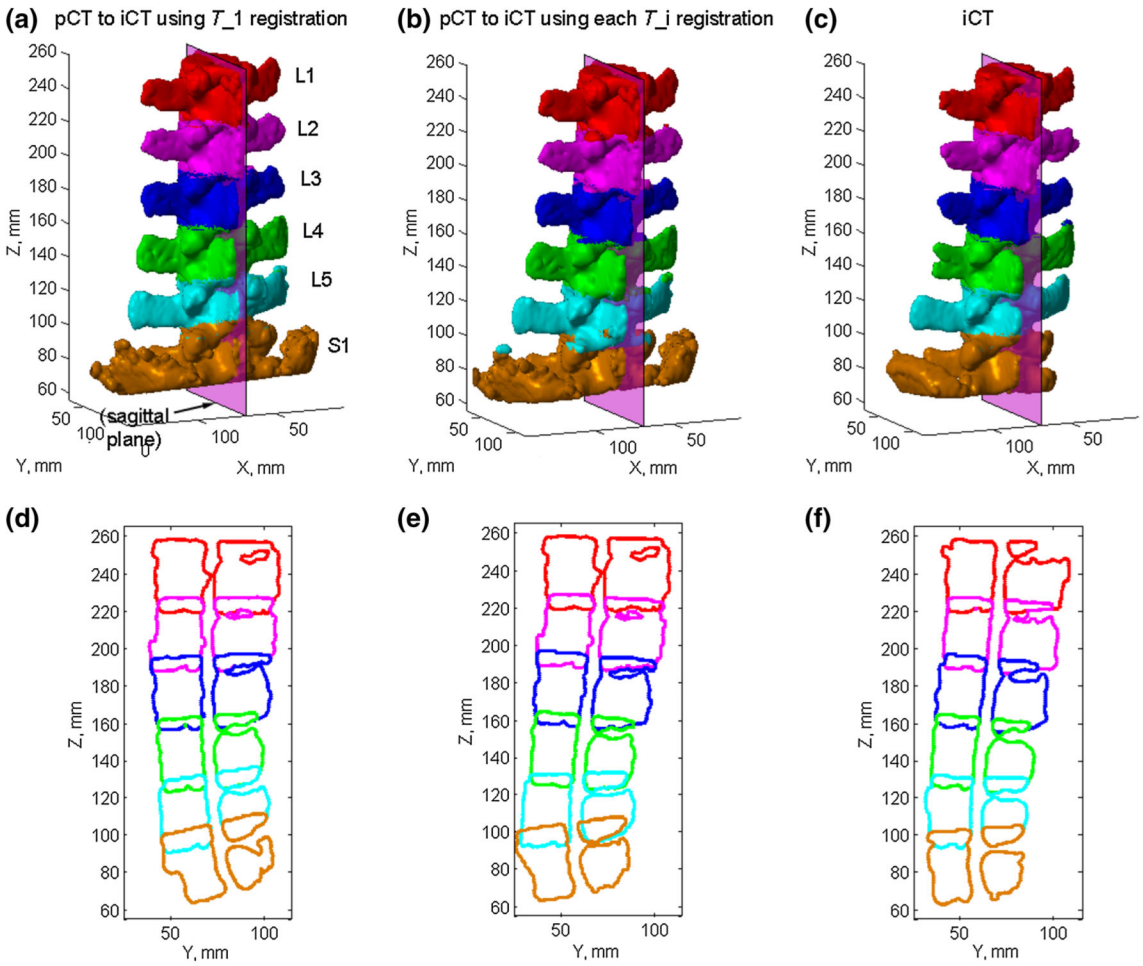

Fig. 9.

Similar comparisons of vertebral poses and sagittal cross sections in pCT and iCT for spine sample #2. Figure caption identical to that in Fig. 8

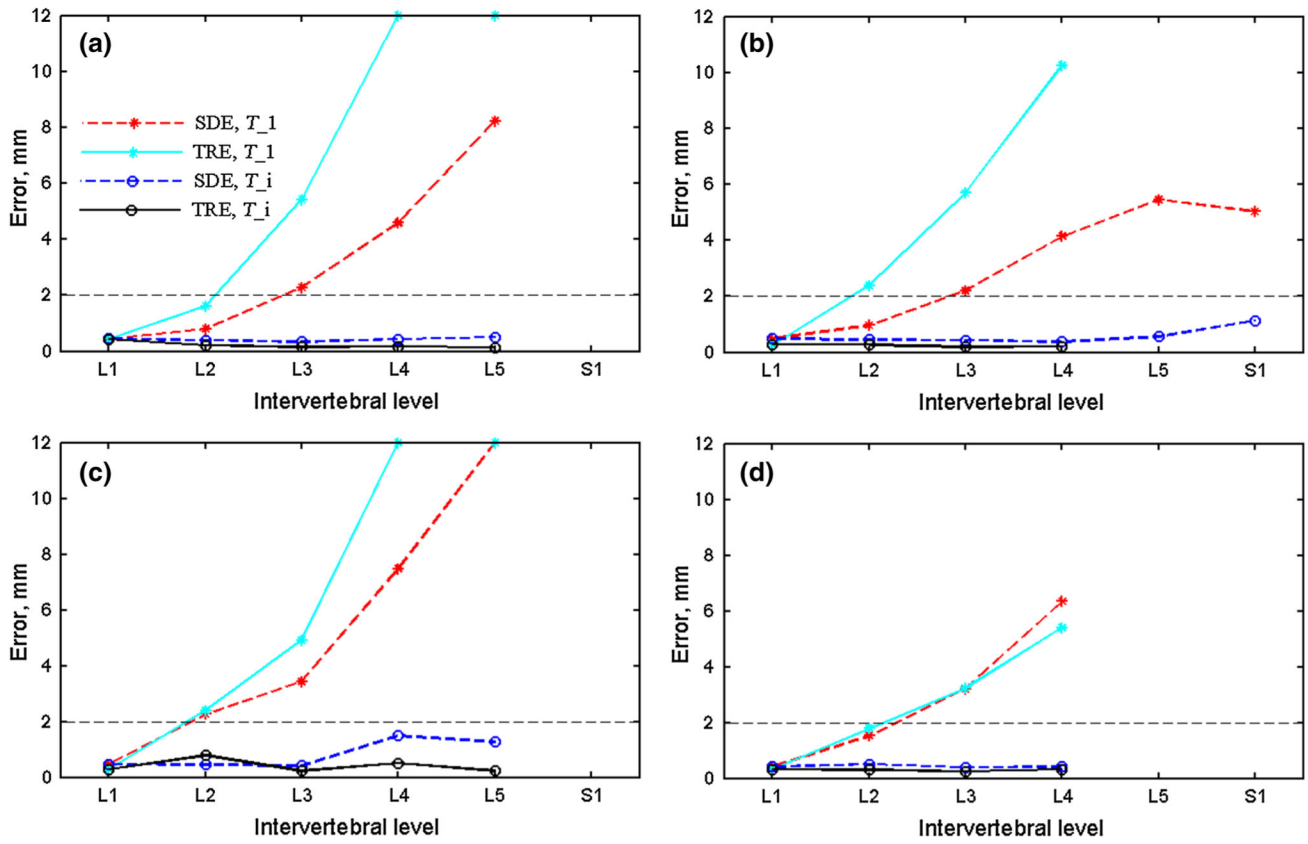

Fig. 10.

SDE and TRE between pCT and iCT registration for each individual vertebra before and after pair-wise registrations (*T*_1 and *T_i*, respectively) for the four samples (**a**–**d**; errors truncated at 12 mm). SDEs/TREs for some vertebrae were not available because either the corresponding segments were not exposed or no screws were implanted

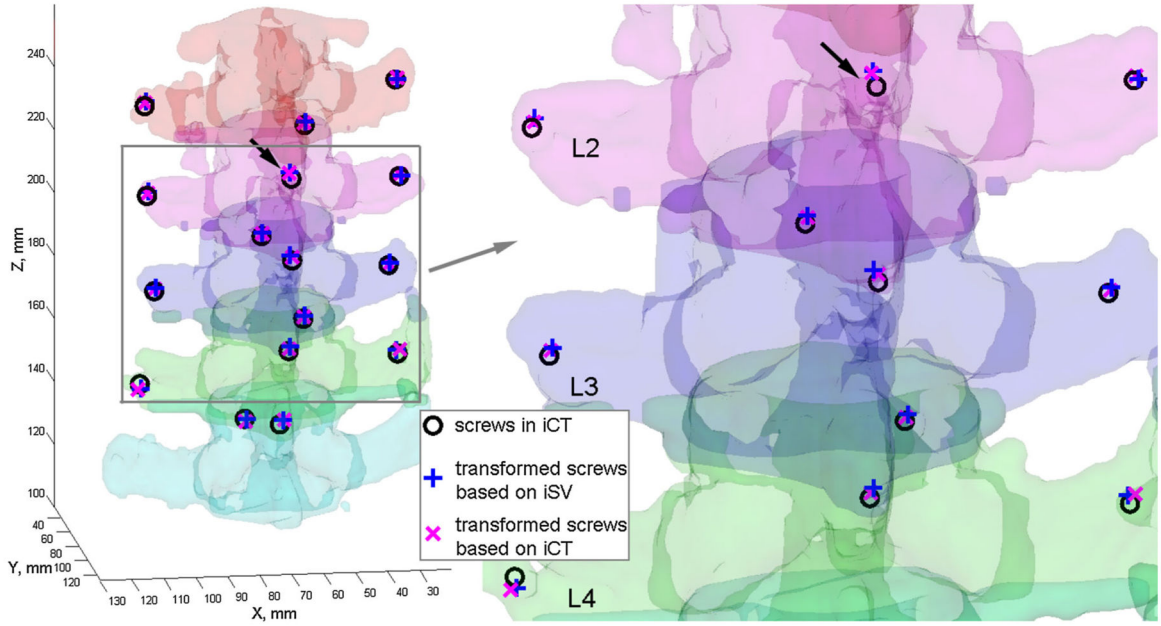

Fig. 11.

Using the individual level registrations obtained from either iSV or iCT, the mini-screw locations in pCT were transformed into iCT. Their close alignments suggest accurate registration from both iSV and iCT. The *arrows* point to the same mini-screw implanted into the spinous process on L2, as identified in Fig. 6

Table 1

Relative intervertebral rotations (in degree) between two adjacent rigid body vertebral segments as recovered from pair-wise registrations at the two neighboring levels

Sample #	L2 → L1	L3 → L2	L4 → L3	L5 → L4	S1 → L5
1	7.24	6.79	4.58	4.91	N/A
2	4.95	2.83	1.54	1.60	3.62
3	7.47	7.71	7.93	6.96	N/A
4	2.98	3.26	3.86	N/A	N/A

Table 2

Summary of individual level registration accuracies using iSV and iCT for intervertebral motion compensation for spine sample #2

Accuracy (mm)	L1	L2	L3	L4	Average (mm)
iSV-based SDE	1.61	1.23	1.20	1.24	1.32 ± 0.19
iSV-based TRE	1.65	1.42	1.29	2.52	1.72 ± 0.55
iCT-based SDE	0.49	0.45	0.43	0.37	0.44 ± 0.05
iCT-based TRE	0.26	0.26	0.20	0.21	0.23 ± 0.03

The iSV reconstruction accuracy before and after inducing the motion was 1.59 and 1.60 mm, respectively, in terms of RMS error between homologous bone-implanted screws identified in iSV and by an independent tracked probe